Suppression of the zero-order diffracted beam from a pixelated spatial light modulator by phase compression

Jinyang Liang,[1,*] Sih-Ying Wu,[1] Fredrik K. Fatemi,[2] and Michael F. Becker[1]

[1]Electrical and Computer Engineering Department, University of Texas at Austin, Austin, Texas 78712, USA

[2]Optical Sciences Division, Naval Research Laboratory, Washington, DC 20375, USA

*Corresponding author: jinyang.liang@mail.utexas.edu

Received 6 January 2012; revised 12 March 2012; accepted 12 March 2012;
posted 14 March 2012 (Doc. ID 161094); published 24 May 2012

Phase compression is used to suppress the on-axis zero-order diffracted (ZOD) beam from a pixelated phase-only spatial light modulator (SLM) by a simple modification to the computer generated hologram (CGH) loaded onto the SLM. After CGH design, the phase of each SLM element is identically compressed by multiplying by a constant scale factor and rotated on the complex unit-circle to produce a cancellation beam that destructively interferes with the ZOD beam. Experiments achieved a factor of 3 reduction of the ZOD beam using two different liquid-crystal SLMs. Numerical simulation analyzed the reconstructed image quality and diffraction efficiency versus degree of phase compression and showed that phase compression resulted in little image degradation or power loss.

OCIS codes: 090.1760, 230.6120, 090.2870.

1. Introduction

Phase-only computer-generated holograms (CGHs), first generated by Lohmann and Paris [1], have been studied intensively to optimize their performance in diffraction efficiency, spatial error, and ease of implementation as a holographic optical element (HOE). For the case of Fourier transform holograms, a target image can be reconstructed at the Fourier plane by using a phase-only optical element. The availability of phase-only spatial light modulators has led to reconfigurable versions of these holographic elements. Various approaches and algorithms have been used to generate phase-only CGHs, including iterative Fourier transforms [2], genetic algorithms [3], and simulated annealing [4]. These developments have let to wide use of phase-only HOEs in various areas, including optical tweezers and beam shaping [5], optical fiber coupling [6], and optical correlators [7]. In many applications, the phase-only HOE is implemented on a pixelated, phase-only spatial light modulator (SLM) for dynamic hologram generation [8]. The incident light on the SLM is modulated by the phase of the pixels and forms the reconstructed image.

However, most of the undiffracted light produces a zero-order diffracted (ZOD) beam on the optical axis at the Fourier plane. The ZOD beam primarily (but not exclusively) comes from the inactive parts of the SLM (e.g., dead space, window reflection, etc.). The ZOD beam poses a difficulty for many applications because of its bright, highly localized nature. Even if the reconstructed image is shifted from the ZOD, this strong source still needs to be prevented from scattering light into the data region. For these reasons, suppression of the ZOD beam is highly desirable when using phase-only SLMs as HOEs.

The usual way to avoid the ZOD beam is to make an in-plane and/or axial translation of the reconstructed image from the ZOD beam. This has been achieved by superimposing both a linear phase

1559-128X/12/163294-11$15.00/0

and a divergent spherical phase [9], or an additional phase checkerboard function [10] to the calculated CGH. As a result, the power of the ZOD beam and target image was redistributed to separate spatial frequencies. However, translation limits the available SLM bandwidth for image encoding. Thus, since the target beam-profile is usually reconstructed at the Fourier plane through a lens, transverse translation can increase the aberration of the resulting image if additional correction terms are not included in the hologram. In addition, undesired power from higher orders of the displayed hologram could be shifted into the region of interest, unless the encoded pattern is oversampled.

A good example of holographic image projection with a suppressed ZOD beam is described by Palima and Daria [11]. They generated an HOE using a variation of the Gerchberg–Saxton (GS) iterative Fourier transform (IFT) algorithm [12] with both amplitude and phase constraints. Their phase-only CGH produced the target beam-profile and a ZOD cancellation beam on the optical axis. The cancellation beam had equal amplitude to the ZOD beam, but with π-shifted phase. As a result, the corrective beam in the reconstructed image destructively interfered with the ZOD beam caused by the less than unity fill factor of the SLM. Later work by Milewski *et al.* [13] used an iterative pixel-by-pixel optimization process for highly precise far-field pattern generation. The optimally designed phase-only HOE considered various characteristic SLM artifacts (e.g., dead space and inter-pixel cross talk) and could be used to cancel a strong unwanted ZOD beam. However, the phase-only CGH suffers from an inherent approximation to fully complex modulation and is therefore limited in achievable precision. Furthermore, adding both amplitude and phase constraints to the numerical algorithm increases the computational complexity and reduces the convergence speed, generally resulting in increased rms error. Finally, these methods require knowledge of the ZOD magnitude before an iterative or minimization algorithm is used to calculate the CGH. As a result, experimental complexity is increased by an additional system for accurate ZOD measurement.

Our objective is to create an easy and quick method to suppress the ZOD beam from holograms produced by phase-only SLMs. Our primary goal is to efficiently suppress the ZOD beam regardless of the precision of the algorithm chosen to create the HOE. In order to overcome problems encountered in previous approaches, the proposed method needs to have a low computational complexity for ZOD suppression and be easily implemented in a phase-only SLM. Most importantly, the ZOD suppression process should not cause significant degradation to the reconstructed image.

In Section 2, we describe the theory of the phase compression technique and show the impact of different parameters affecting the phase distribution in phase-only HOEs that are designed to suppress the ZOD beam. Section 3 presents the experimental results of ZOD beam suppression using two different phase-only liquid-crystal SLMs. The hologram quality and diffraction efficiency for different phase compression factors are examined using numerical simulation in Section 4, and a summary concludes this paper in Section 5.

2. Theoretical Analysis of the Phase Compression Technique

The problem is posed in the following way. Figure 1 shows the optical layout of the phase compression experiment for a Fourier transform CGH. The collimated input laser beam of wavelength λ is incident on a phase-only pixelated SLM. The active area has a rectangular aperture $b(\xi,\eta)$. Each square pixel has pitch d and length a. The active area of the pixels divided by the total SLM area is defined as the area fill factor, $ff = (a/d)^2$. The 2D discrete CGH, $\exp[jp_h(\xi,\eta)]\mathrm{comb}(\frac{\xi}{d},\frac{\eta}{d})$ is encoded onto the SLM, where $p_h(\xi,\eta)$ is the phase angle calculated for the CGH. To account for curvature of the SLM chip, $p_{\mathrm{SLM}}(\xi,\eta)$ is the smooth and continuous phase angle introduced by the SLM surface shape. It applies to every part of the SLM, and in conjunction with the rectangular amplitude function $b(\xi,\eta)$ gives the complex reflectance across the SLM aperture when it is inactive.

The target image is reconstructed at the back focal plane of a Fourier lens with focal length f. The field at the Fourier transform plane consists of replicas of the reconstructed hologram centered at the SLM pixel diffraction orders. The strong, centermost replica is of interest to our study and occupies the range $\pm\lambda f/2d$ in the x-y coordinate plane. This region contains the reconstructed image, the ZOD beam at the orign, and the conjugate reconstructed image, if it exists.

In the far field, the ZOD beam represents the dc term of the Fourier transform of the SLM's phase pattern plus any specular reflected light from the SLM or its window. The shape of the ZOD from the SLM pixel area is determined by the aperture function, $b(\xi,\eta)$, and any distribution of phase or amplitude from non-modulated region(s). Therefore, the optical field of the ZOD beam at the centermost region can be written as

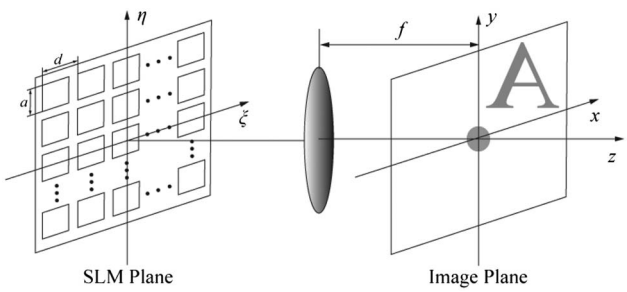

Fig. 1. Optical layout of the phase compression experiment. Pixelated SLM is in the ξ–η coordinate system, and the holographic image is reconstructed at the x-y coordinate plane.

$$U_{\mathrm{zod}}(f_x,f_y) = \{[A_{\mathrm{zod}}\exp(j\phi_{\mathrm{zod}})]\delta(f_x,f_y)\} \otimes M(f_x,f_y), \quad (1)$$

where A_{ZOD} and ϕ_{ZOD} are the amplitude and phase of the ZOD beam in the far field, respectively, and $\otimes$ is the convolution operator. Spatial frequency at the image reconstruction plane is represented by $f_x = \frac{x}{\lambda f}, f_y = \frac{y}{\lambda f}$. In the far field, the ZOD delta function is convolved with the frequency domain representation of both the aperture function and SLM phase curvature so that $M(f_x f_y)$ can be written as $M(f_x,f_y) = F\{b(\xi,\eta)\exp[jp_{\mathrm{SLM}}(\xi,\eta)]\}$, where $F\{\}$ denotes the 2D Fourier transform. Therefore, if we can produce additional undiffracted light in the hologram reconstruction with equal amplitude, π-shifted phase, and the same functional form as the undiffracted ZOD light given in Eq. (1), then the ZOD beam can be suppressed by destructive interference.

We propose to apply the phase compression technique following the CGH design in order to suppress the ZOD beam. Whereas other techniques apply ZOD suppression as part of the CGH design, our technique applies it afterwards and hence does not require recomputation of the CGH or interfere with the operation of the CGH algorithm. The phase angle of each pixel in the derived CGH is modified by the following equation:

$$p_c(\xi,\eta) = [cp_h(\xi,\eta) + (\pi + \phi_{\mathrm{zod}})] \pm 2\pi m, \quad (2)$$

where c is the phase compression factor, $0 < c \le 1$, and $p_c(\xi,\eta)$ is the pixel phase angle after compression. The integer m confines the compressed phase angle to within a 2π range (modulo 2π).

The process of phase compression is illustrated using the phase histogram and complex unit-circle diagrams in Fig. 2. First, the designed CGH $p_h(\xi,\eta)$ has the uniform phase angle distribution shown in Fig. 2(a). On the complex plane, this distribution can be represented by a full unit-circle. Phase compression changes the phase distribution in the histogram to $p_c(\xi,\eta) \in [-c\pi\, c\pi]$, as shown in Fig. 2(b). This corresponds to an open arc on the unit-circle. As a result, the summation of all CGH pixels forms a sum vector pointing to zero phase angle (i.e., on the real axis), as shown in Fig. 2(c). Second, a uniform phase angle, $\theta = \pi + \phi_{\mathrm{zod}}$, is added into the entire CGH to create the π-shifted phase with respect to the ZOD beam. This is shown as the rotation angle θ in Fig. 2(d). The resulting rotated sum vector is used as the ZOD cancellation beam.

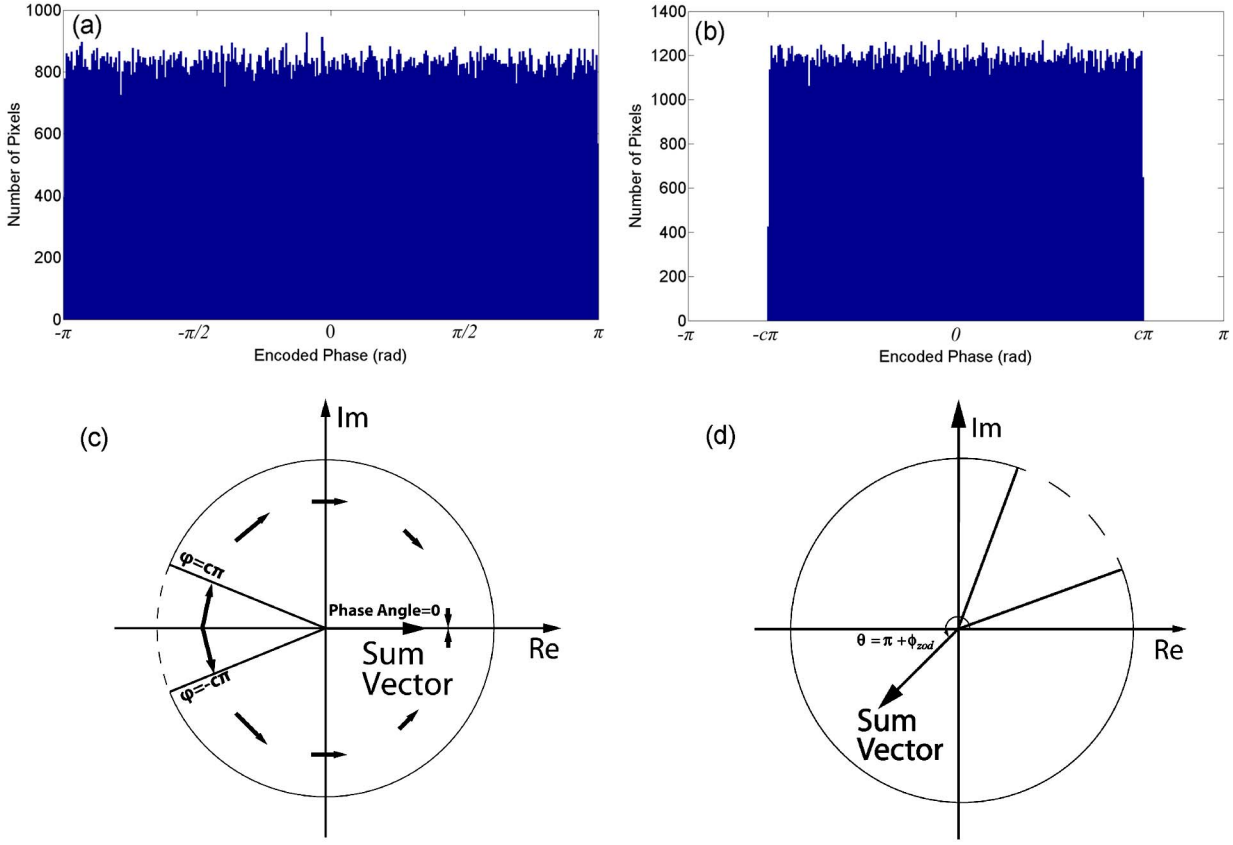

Fig. 2. (Color online) Representation of the phase compression technique: (a) uniformly distributed phase angle histogram of the CGH after the IFT algorithm; (b) phase compression redistributes the phase angle of the CGH pixels, $P_h(\xi,\eta) \times c$, as shown; (c) phase distribution, same as (b), on the complex unit-circle after phase compression; complex vectors sum up to create the ZOD cancellation vector at zero phase; (d) rotation angle, $\theta = \pi + \phi_{\mathrm{zod}}$, determines the phase of the resulting corrective vector.

The phase compression factor c determines its amplitude, and the rotation angle θ, its phase.

The following theoretical analysis shows ZOD suppression using phase compression. At the SLM plane (continuous ξ–η coordinate system), the transmission function from the active pixels, $u_a(\xi,\eta)$, is given by the discrete pixel phase multiplied by the SLM aperture and surface phase function:

$$u(\xi,\eta) = u_a(\xi,\eta)[b(\xi,\eta)\exp(jp_{\mathrm{SLM}}(\xi,\eta))], \tag{3}$$

where the discrete pixel phase is given by

$$u_a(\xi,\eta) = \left\{\exp[jp_h(\xi,\eta)]\mathrm{comb}\left(\frac{\xi}{d},\frac{\eta}{d}\right)\right\} \otimes \mathrm{rect}\left(\frac{\xi}{a},\frac{\eta}{a}\right),$$

and where

$$\mathrm{rect}\left(\frac{\xi}{a},\frac{\eta}{a}\right) = \begin{cases} 1, & (-a/2 < \xi,\eta < a/2) \\ 0, & \text{otherwise} \end{cases},$$

$$\mathrm{comb}\left(\frac{\xi}{d},\frac{\eta}{d}\right) = \sum_{m=-\infty}^{\infty}\sum_{n=-\infty}^{\infty}\delta(\xi - md, \eta - nd).$$

At the lens focal plane, the image reconstruction field from the CGH pixels can be described by the Fourier transform of Eq. (3). The image reconstruction field is therefore given by

$$U(f_x,f_y) = U_a(f_x,f_y) \otimes M(f_x,f_y), \tag{4}$$

where

$$U_a(f_x,f_y) = ff\left[P_h(f_x,f_y) + \sum_{m,n\neq 0} P_h\left(f_x - \frac{m}{d}, f_y - \frac{n}{d}\right)\right]\mathrm{sinc}(af_x, af_y) \tag{5}$$

is the Fourier transforms of $u_a(\xi,\eta)$. The pixel shape factor takes the form of a sinc function, which is defined by $\mathrm{sinc}(af_x,af_y) = [\sin(\pi af_x)/\pi af_x] \times [\sin(\pi af_y)/\pi af_y]$. The Fourier transform of the *comb* function is $F\{\mathrm{comb}(\frac{\xi}{d},\frac{\eta}{d})\} = \frac{1}{d^2}\mathrm{comb}(df_x,df_y)$ and satisfies conservation of energy. The reconstructed target image amplitude is the Fourier transform of the phase-only CGH, $P_h(f_x,f_y) = F\{\exp(jp_h(\xi,\eta))\}$. In the derivation, we dropped the quadratic phase factor that depends on the SLM-lens separation [14], because it is independent of the CGH design and has the same impact on the ZOD beam and on $U_a(f_x,f_y)$.

The total reconstructed field is the sum of the hologram and ZOD contributions. The total amplitude is written by combining the Eq. (5) with Eq. (1) to obtain

$$U_0(f_x,f_y) = \left\{A_{\mathrm{zod}}\exp(j\phi_{\mathrm{zod}})\delta(f_x,f_y) + ff\left[P_h(f_x,f_y) + \sum_{m,n\neq 0} P_h\left(f_x - \frac{m}{d}, f_y - \frac{n}{d}\right)\right]\mathrm{sinc}(af_x,af_y)\right\} \otimes M(f_x,f_y). \tag{6}$$

The ZOD beam is the first term with the delta function, and the convolution with $M(f_x,f_y)$ defines its shape. Thus, our primary goal becomes how to manipulate the CGH to produce a ZOD cancellation beam with correct amplitude, phase, and functional form to fully suppress the ZOD beam, given by $[A_{\mathrm{zod}}\exp(j\phi_{\mathrm{zod}})\delta(f_x,f_y)] \otimes M(f_x,f_y)$.

Based on Huygens–Fresnel diffraction, all pixels in the SLM plane contribute to the interference on the optical axis. As a result, the amplitude and phase angle of the ZOD cancellation beam is determined by the summation of all pixels in the CGH. In essence, the purpose of phase compression is to create a sum vector pointing in the opposite direction from ϕ_{zod} with identical magnitude.

After phase compression, the modified CGH produces the target image with the ZOD cancellation beam, and Eq. (6) becomes

$$U_{0C}(f_x,f_y) = \left\{(A_{\mathrm{zod}} - A_c)\exp(j\phi_{\mathrm{zod}})\delta(f_x,f_y) + ff\left[P_i(f_x,f_y) + \sum_{m,n\neq 0} P_h\left(f_x - \frac{m}{d}, f_y - \frac{n}{d}\right)\right]\mathrm{sinc}(af_x,af_y)\right\} \otimes M(f_x,f_y). \tag{7}$$

We assume that the dc component (the ZOD cancellation beam) at the origin arising from the phase compressed hologram pixels ($-A_c$) comes primarily from the dc component of the $m = n = 0$ term of the sum and that the higher-order terms make negligible contribution at the origin. Thus we can separate the dc component from $P_h(f_x,f_y)$, and the remainder becomes $P_i(f_x,f_y)$. The first term in Eq. (7) represents the suppressed ZOD beam with amplitude $(A_{\mathrm{zod}} - A_c)$. By examing Eq. (7), we see that the ZOD cancellation beam has the same functional form as the ZOD beam , but with a π-shifted phase. Thus, these two beams always have the same functional form and always destructively interfere. In addition, we see that the ZOD is fully canceled when $A_{\mathrm{zod}} - A_c = 0$.

Phase compression is a subset of a more general phase scaling effect (i.e., includes both phase compression and phase expansion) that has been studied mainly in diffractive optics. For instance, in the design and fabrication of diffractive optical elements, the phase scaling effect is often known as the phase depth error due to imprecise fabrication depth control [15,16]. In addition, it has been studied in multiwavelength holographic image projection where the hologram designed for one wavelength appears as a scaled phase for the other wavelengths [17]. Phase

scaling error produces extra noise in the reconstructed image and reduces the diffraction efficiency by introducing an on-axis component (i.e., extra ZOD beam) [18]. The phase scaling effect is detrimental in these examples. However, with the phase-only SLM, we introduced a π-phase shift after phase scaling. As a result, the introduced ZOD beam that arises due to phase scaling destructively interferes with the unwanted ZOD beam from other sources.

We derived the amplitude of the ZOD cancellation beam A_c from the phase compression factor and SLM area fill factor. The aim is to sum (integrate) the on-axis contribution from all the pixels to the dc component at the hologram reconstruction plane. From the phase histogram of the hologram, the phase is approximately uniformly distributed in the range of $[-c\pi, +c\pi]$ after compression. Therefore, the distribution density function (pixels/unit-phase-angle) is given by $\rho(\theta) = \frac{N}{2\pi c}$ where N is the total number of SLM pixels. Before compression, the density function was $N/2\pi$.

The phase of any SLM pixel can be represented by $\exp(j\theta) = \cos\theta + j\sin\theta$. The phase distribution histogram (Fig. 2(c)) shows that the phase distribution is symmetric about the *real* axis, meaning that the imaginary part can always be canceled by its complex conjugate. As a result, the integral of the imaginary part of the phase distribution is zero. However, the phase distribution is not symmetric with respect to the *imaginary* axis, meaning that the real parts of all the phases cannot totally cancel. This, in fact, is the origin of the ZOD cancellation beam. Assume the input laser source has a uniform amplitude $A_i = 1$, the sum of the real part (integral in continuous variables) of all the pixel's contributions to the dc spot becomes

$$A_c = A_i ff \int_{-\pi c}^{\pi c} \rho(\theta)\cos\theta \mathrm{d}\theta = Nff\frac{\sin(\pi c)}{\pi c}. \quad (8)$$

In order to fully cancel the ZOD beam, we must have $A_{\mathrm{zod}} = A_c$. Therefore, we get

$$\mathrm{sinc}(c) = \frac{A_{\mathrm{zod}}}{Nff}\ (0 < c \le 1). \quad (9)$$

Equation (9) can be used to estimate the degree of phase compression required to compensate a given SLM fill factor. The amplitude of the ZOD cancellation beam can be manipulated by controlling the phase compression factor. Thus, we have satified all three conditions for ZOD beam suppression (correct amplitude, π-shifted phase, and identical functional form). It is expected that the ZOD beam from the SLM can be strongly suppressed.

Phase compression redistributes power from the on-axis ZOD beam to the higher diffraction orders. The high-order replicas produced by the pixelated SLM are also found for certain sources of ZOD beams. For instance, the ZOD contributions from the dead space or from the smooth transition region between SLM pixels have high-order replicas. Based on the theoretical derivation, the ZOD beam in these high orders has a π-phase difference from the ZOD beam on the optical axis. On the other hand, phase compression does not change the phase of the reconstructed images in higher diffraction orders. As a result, when ZOD cancellation destructively interferes with the ZOD beam on the optical axis, it constructively interferes with the ZOD beams in the higher diffraction orders. Thus, the energy of the ZOD beam on the optical axis is redistributed to the higher diffraction orders.

Compared to previously reported methods [11,13], our method does not have any additional phase and amplitude constraints in the CGH design process. Suppression of the ZOD beam starts from the precomputed hologram and is accomplished by adjusting two parameters (c and θ). Finding a minimum for the ZOD by experimental adjustment is easy since the functional form of the suppressed ZOD power versus c and θ derives from interference, so the variables are separable, and there is a single-value minimum (modulo 2π). We can quickly find this minimum though global adjustment and do not need to redesign the hologram for each case. Thus, any algorithm can be used to achieve an optimized CGH since phase compression is applied after the CGH is designed. This significantly reduces the computational complexity for the ZOD suppression process.

A significant consideration is that the phase angles in the CGH have been changed from $p_h(\xi,\eta)$ to $p_c(\xi,\eta)$ by the phase compression process. We need to demonstrate that this change does not significantly degrade hologram reconstruction and to quantify the introduced error. We will next show experimental results for ZOD suppression by phase compression in Section 3 and then discuss the reconstructed hologram quality after phase compression using the simulations presented in Section 4.

3. Experimental Results

A. SLM with 100% Fill Factor

Tests with two different SLMs were conducted to demonstrate the phase compression technique. First, we used a reflective nematic liquid-crystal SLM (Boulder Nonlinear Systems P512-0785) with 512×512 resolution and 15 μm pixel size (7.68×7.68 mm^2 active area). The experiment used a 780 nm laser source that matched the SLM design wavelength. The active area is covered by a flat dielectric mirror to achieve 100% fill factor for this device. However, this process cannot completely eliminate the optical grating effect caused by the pixel structure. Because of the dielectric mirror, the abrupt change in phase modulation between active pixels (i.e., dead space) is reduced to a smooth transition region from one pixel to the next [19]. Normally, the phasor sum of the contributions from of all these transition regions will not be zero, and thus they will make a small contribution to an on-axis ZOD beam

[20]. The reason for this derives from the CGH design that will randomly distribute the pixel phase angles from $-\pi$ to $+\pi$. Most iterative algorithms will do this naturally, and the result will be that the Fourier transform hologram has no dc spot on axis. This is not necessarily true for the transition regions. If the phase is encoded modulo 2π on the SLM, each transition must span two phase values and have a phasor sum angle near the mean of the two adjacent pixel phase angles. This results in a histogram of the phases from all the transition regions over the SLM that is lower at the ends (at $-\pi$ and $+\pi$) than at the center. The sum of all the phasor contributions at an on-axis point from the entire hologram cannot now sum to zero. However, additional CGH design measures can still be taken to eliminate this source for a ZOD beam. Thus, we conclude that this SLM will produce a ZOD and that the methods and analysis for suppressing this ZOD by phase compression can be legitimately employed.

The experimental setup is shown in Fig. 3. A collimated Gaussian beam with $1/e^2$ radius $w_0 = 10.0$ mm was passed through a circular aperture with diameter 7.0 mm to provide roughly uniform intensity to the SLM. The beam polarization was set to vertical (active axis of the SLM) by a Glan Thompson polarizer with 10^5 extinction ratio. The SLM was tilted by 100 mrad to separate the diffracted and ZOD beams from the incoming beam. The reflected beams were collected by a 75 mm achromatic lens, and the images were captured by a 1280×960 CCD camera (Sony DMK 41BU02). The CCD was at the back focal plane of the lens to capture a far-field diffraction patter scaled to fit the camera sensor. The SLM was not at the lens front focal plane and thus introduced quadratic phase terms multiplying the Fourier transform. However, the image is still the correct magnitude squared of the Fourier transform and correctly represents the reconstructed holographic image.

B. Experimental Method and Results

In the experiment, both the ZOD beam and high-order replica are observed for this SLM. We applied HOEs corresponding to the desired target images to the SLM. These phase profiles were determined by the GS algorithm [12]. To show how phase compression can be used easily and quickly with adaptive adjustment methods, the optimum values of c and θ were found as follows. First, the phase compression factor c was set to achieve the best ZOD suppression. Then the constant phase θ that is added to each pixel was adjusted to minimize the ZOD. Since c and θ are global parameters over the SLM face, they may be quickly adjusted without having to recompute the HOE.

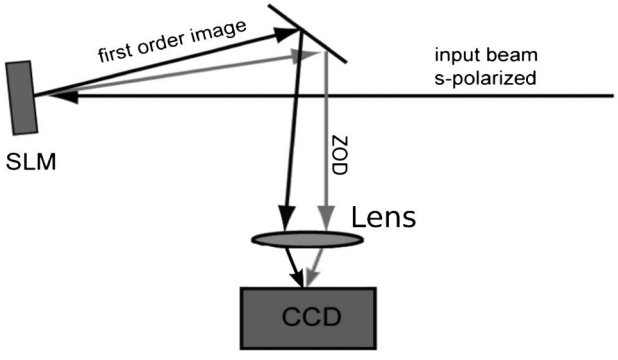

Fig. 3. Experimental setup for phase compression tests with lens focused to place the focal plane at the CCD surface.

In the experiment, we created a series of HOE phase profiles using Eq. (2), with $c = 0.60$ to 1.00. The power in the zeroth diffraction order domain (x, y within $\pm\lambda f/2d$) for the ZOD spot and the power in the reconstructed image were each integrated. The normalized ZOD power is plotted in Fig. 4 as a function of compression factor and rotation angle θ. Figure 4(a) shows the zero-order power as a function of c, and a minimum at $c = 0.80$ that is about 3 times lower than for $c = 1.00$. For this plot, the rotation angle θ was fixed at 180°. The ZOD beam power as a function of θ is shown in Fig. 4(b), with c adjusted as shown above for a minimum. For this SLM, there was no further improvement when varying these parameters.

In addition, we found that the reconstructed image of the letter "A" did not observably change. In order to

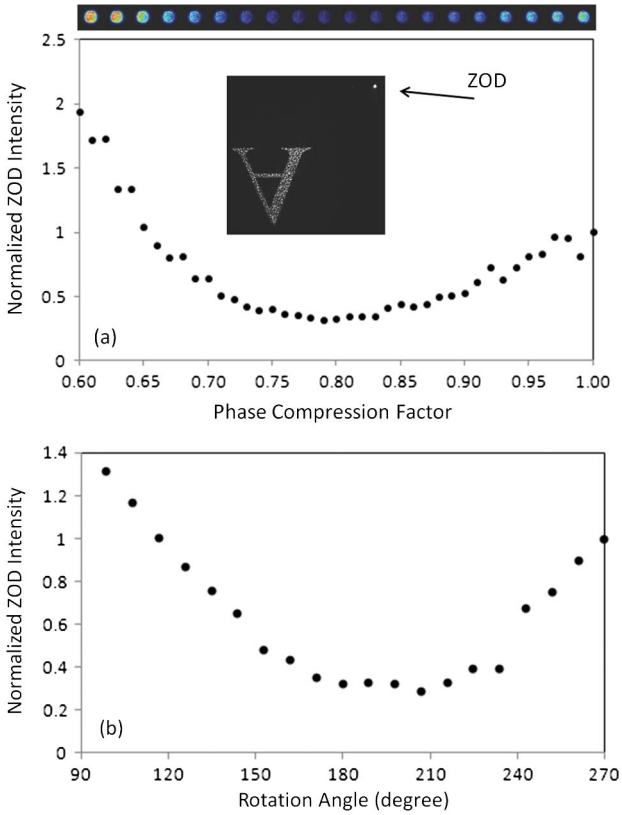

Fig. 4. (Color online) ZOD suppression measurement using the BNS P512–0785. Normalized diffracted power of the ZOD beam versus (a) phase compression factor with experimental images of the ZOD beam evolution (inset above) and reconstructed image (inset middle), and (b) rotation angle with $c = 0.8$. The data is normalized by the ZOD intensity for $c = 1.0$ and $\theta = 180°$.

quantify the quality of holographic image reconstruction, we calculated the signal-to-noise ratio (SNR) of the reconstructed image with respect to the original target image intensity in the image area. For the reconstructed images before and after phase compression, the total image power (sum of pixel magnitude squared in the image area) was equalized to that of the target image. The SNR was calculated by

$$\mathrm{SNR_{dB}} = 10\log_{10}\left(\frac{\sum(|A_t(f_x,f_y)|^2)^2}{\sum(|A_o(f_x,f_y)|^2 - |A_t(f_x,f_y)|^2)^2}\right), \tag{10}$$

where A_o and A_t are the amplitude of the reconstructed image and of the target image, respectively, with equalized image power.

The resulting SNR for the region of the letter "A" was 1.75 dB, both before and after phase compression. The low SNR was mainly due to the speckle effect in the hologram reconstruction. This result also illustrated that experimental noise sources in the image, such as coherent speckle noise, dominated the noise level from the design algorithm and phase compression.

C. Analysis

Although the qualitative features of the technique were clearly demonstrated by this SLM, the ZOD could not be completely eliminated due to the various other contributions to the ZOD by a typical SLM. For instance, reflections from the front and back surfaces of the protective cover glass would result in one or two spots in the focal plane, depending on its tilt and wedge angle. Furthermore, differences in shape between the SLM surface and the cover glass surfaces could shape these spots differently.

Although c compresses the phase applied to the SLM, nonlinearities and calibration errors in the SLM lookup table (LUT) can produce quantitative differences from the simulation. The LUT can also vary slightly from pixel to pixel. The integrated power diffracted into the reconstructed image is shown in Fig 5. Note that the diffracted power changed little between $c = 0.8$ and $c = 1.0$, whereas the simulation showed that the power should have changed by 8%. The power also peaks slightly for $\theta = 180°$, whereas ideally it should be constant with respect to the rotation angle. These results also suggest calibration errors in the SLM. In this range of c, however, the ZOD power was reduced by more than a factor of 3. We observed that the power in the ZOD was much lower than the total power in the reconstructed image, so a variation of 3 times in the ZOD resulted in a smaller fractional change to the power of the reconstructed image.

The variations from ideal behavior noted above come from the non-ideal modulation of the SLM and the lack of a LUT for each pixel. The diffraction efficiency of a nematic SLMs is typically dependent on the spatial frequency of the SLM phase profile. This is because the pixels are not completely isolated from one another, and voltages controlling the phase on one pixel perturbed the adjacent pixels. This nonzero transition distance between pixels has two effects when large pixel-to-pixel phase changes are desired. First, the effective fill factor is reduced because light in the transition region for large phase changes is diffracted outside the imaging system. Second, the depth of phase modulation is reduced (i.e., the modulation transfer function of the SLM decreases at higher spatial frequencies). For this latter effect, phase changes in regions of high spatial frequency are already compressed and would thus require recalibration. So in real devices with finite transition regions, areas of high spatial frequency or large phase changes require different compression factors to be applied. We measured the diffraction efficiency of this SLM as a function of spatial frequency by applying a blazed grating function $\phi = 2\pi(x/N)D$, where $N = 512$ is the pixel count, $1 \le x \le N$, and D is the grating frequency (e.g., for $D = 64$ cycles across the SLM, the period is $N/D = 8$ pixel). To extract the effect of spatial frequency from other parameters (e.g., the 70% reflectivity of the SLM), we define diffraction efficiency here as the power into the first order divided by the total reflected power. Our measured diffraction efficiencies into first order were 0.96, 0.92, 0.75, and 0.34 for $D = 32$, 64, 128, and 256 (the Nyquist frequency), respectively. The theoretical

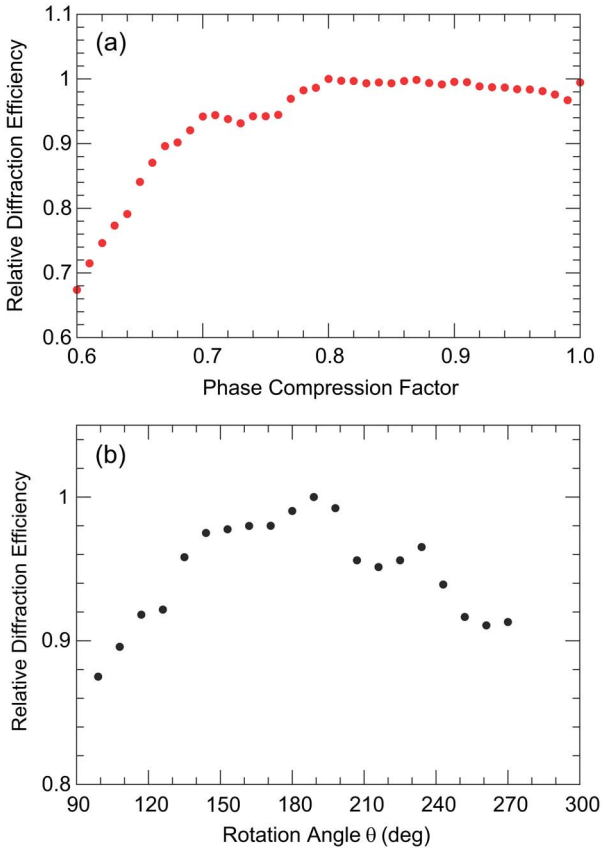

Fig. 5. (Color online) Diffraction power of the reconstructed image versus (a) phase compression factor c and (b) phase rotation angle θ.

diffraction efficiencies at these respective spatial frequencies are 0.99, 0.95, 0.82, and 0.41. Note that at the Nyquist frequency, we achieve only 83% of the theoretical value, but at the lowest spatial frequencies, we achieve 97% of the theoretical value. We attribute this to the increased effect of finite transition regions that diffract light away from the target order. So our SLM showed some degree of reduced modulation transfer function at the highest spatial frequencies. Thus, the deviation from positive slope in Fig. 5(a) between $c = 0.8$ and 1.0 and the lack of flatness for diffraction efficiency versus θ in Fig. 5(b) are likely due to these uncompensated deviations from ideal behavior in the SLM.

D. SLM with Limited Fill Factor

In a second experiment, a reflective liquid-crystal SLM (Boulder Nonlinear Systems P512-1064) with 512×512 resolution and 15 μm pixel size (7.68×7.68 mm^2 active area) was tested by a similar experimental setup with an exact Fourier plane dxetection (SLM and camera are placed at the front and back focal plane of the lens). This device had a fill factor of 83.5% [21]. A He–Ne laser with 633 nm wavelength was used in this experiment. The expected phase compression factor for a SLM with dead space can be derived from the fill factor by using Eq. (8), as $c = 0.828$ with $A_{\text{zod}} = 1 - ff$.

The possible phase modulation depth of the BNS SLM (P512-1064) was much larger than 2π at 633 nm than at its design wavelength of 1064 nm. As a result, using the 633 nm wavelength avoided the possibility of shallow ($<2\pi$) modulation depth and guaranteed a full 2π modulation range, which is important for optimum performance of the phase compression process. LUT measurement showed that the modulation depth of this device ranged from 0 to 2.7 ($\times 2\pi$) at 633 nm. We extracted a region with 2π modulation depth that utilized the largest number of digital number steps and left the remaining digital numbers unused. The hologram designed by the IFT was mapped to this extracted LUT and loaded onto the SLM. When the SLM was operated in this way, no extra power was sent to the ZOD beam due to phase scaling effects, and the measurement results are representative of phase modulators with dead space.

The optimum experimental values of c and θ were found by using the same method described in Subsection 3B. First, we scanned the rotation angle with $c = 0.95$ and found the optimum angle was $\theta = 10°$. Second, the angle was fixed while different phase compression factors were applied and the maximum ZOD suppression was found at $c = 0.79$. No further improvement was obtained by scanning the rotation angle again. Experimentally measured scans of normalized ZOD power versus phase compression factor and rotation angle are shown in Fig. 6. The experiment produced a minimum ZOD power that was 3 times lower than for $c = 1.0$. Because the antireflection coating on the SLM cover window did not match the operation wavelength, an additional ZOD beam from window reflection was observed in this experiment. As a result, the actual phase compression factor was smaller than the theoretical value. This experimental result demonstrates that we can efficiently suppress the ZOD caused by various sources, but different functional forms for these beams may cause non-uniform suppression and leave some residual ZOD power.

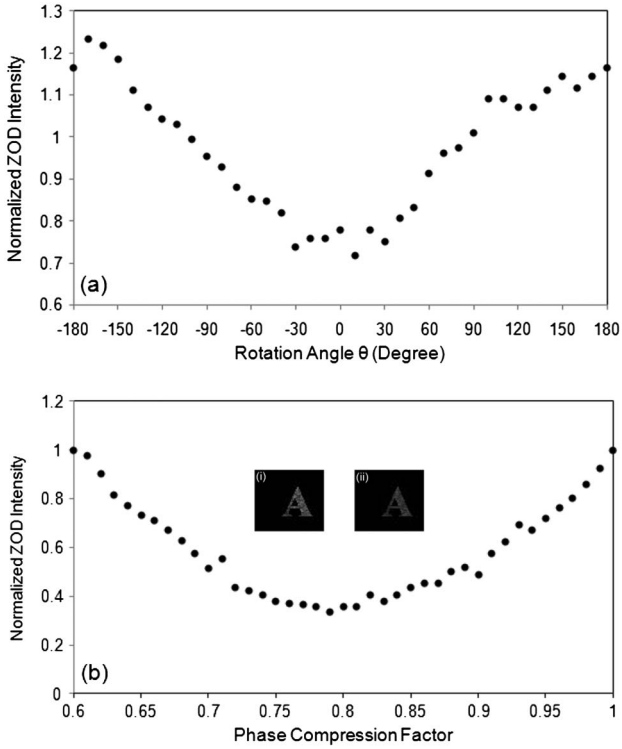

Fig. 6. ZOD suppression measurement using the BNS P512–1064. Diffracted power of ZOD beam versus (a) phase compression factor with $c = 0.95$ and (b) rotation angle with $\theta = 10°$. The extracted region of letter "A" from reconstructed images for (i) $c = 1.0$ and (ii) $c = 0.79$ are inset into (b). The data is normalized by the ZOD intensity for $c = 1.0$ and $\theta = 10°$.

4. Simulation Results

Because experimental results showed an unobservable change in the SNR of the reconstructed image after phase compression, it was difficult to investigate the change of hologram quality from phase compression exclusively. Therefore, a numerical simulation was conducted to examine the hologram quality in terms of image fidelity and diffraction efficiency. First, we investigated the degree of image degradation induced by phase compression. Four different target images were tested in this simulation, and their properties are summarized in Table 1. Each target image was zero-padded in a 512×512 pixel field and offset from the center. The SLM area fill factor was set at 0.9, and the phase introduced by the dead space was $\phi_{\text{zod}} = 0$.

We used a two-step process to eliminate the ZOD beam and to simulate the reconstructed image; its

Table 1. Summary of the Properties of the Four Test Images

Test Image	Size (pixels)[a]	Type	Image
Letter "A"	90 × 90	Binary, character	
Dog	182 × 182	Grayscale, image	
Square	128 × 128	Binary, solid area	
Dots Array[b]	256 × 256	Binary, beam fan-out	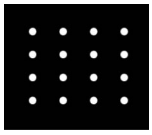

[a]All target images are padded into a512 × 512 array.
[b]The dots array is a 4 × 4 array of 1-pixel spots with 50-pixel spacing (the dots are exaggerated for visibility in the image).

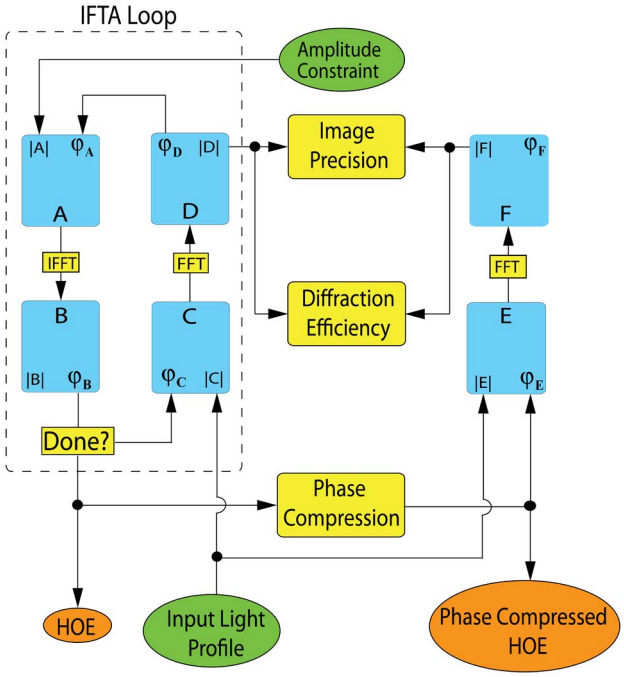

Fig. 7. (Color online) Flowchart of the phase compression technique using the IFT algorithm (IFTA) and the quality comparisons of the reconstructed images.

flow chart is shown in Fig. 7. First, the CGH was derived by an IFT algorithm (IFTA). As a phase-retrieval algorithm, the IFTA simulated light propagating and counter-propagating between the HOE (object) and reconstructed image (target) planes as shown on the left in Fig. 7, at the bottom and top of the loop, respectively. The algorithm forces the desired amplitude condition at the object plane and applies amplitude and/or phase constraints at the target image plane while allowing the phase to evolve. The designed phase-only CGH therefore produced the desired target beam-profile with some residual error after the IFTA converged. We used both the GS algorithm [12] and the modified adaptive-addictive (AA) algorithm [22] to compare image degradation of phase compressed holograms designed by different algorithms.

The second process step was to apply different phase compression factors with $p_{\mathrm{SLM}}(\xi,\eta) = 0$ for a perfectly flat SLM surface. The quality of holographic image reconstruction was determined by the difference in SNR (Eq. [9]) between the reconstructed image and the original target image for the entire diffraction field. The SNR versus phase compression for the test images using the GS algorithm is plotted in Fig. 8(a). The starting value of rms error at $c = 1.0$ was indicative of how well the GS algorithm performed and was seen to vary for different target images, depending on the area of the 512 × 512 field covered by the image and on the specific image content. Since compression redistributed the phase angles of the HOE pixels, we expected this technique would introduce some by-products, such as a conjugate image and background noise. The generated noise degrades the reconstructed image quality and reduces the SNR. Most relevant for using phase compression with an HOE using a typical SLM was the fact that a reasonably good SNR was maintained for a wide range of c. For typical liquid-crystal SLMs, the phase compression factor to fully suppress the ZOD beam falls in the range of $c = 0.80$ to 0.95 for fill-factor, $ff = 81.1\%$ to 95.0%. The image SNR was decreased by 1.5 to 2.8 dB (for $c = 0.80$) for different target images, indicating that the hologram quality would be preserved for these realistic cases.

The effect of phase compression on hologram reconstruction fidelity can be understood by the following argument. Phase compression (without phase angle rotation) will not change the hologram fringe spacing but slightly reduce the phase modulation depth. Phase angle rotation will manifest as a lateral shift of less than one fringe period that will leave fringe amplitude and period unchanged. This suggests why phase compression with $0.8 \le c \le 1.0$ has such a minimal effect on the reconstructed image quality. A linear reduction in modulation depth will be expected to reduce the diffraction efficiency, but since the phase fringes are not distorted and a linear (but compressed) mapping of modulation phase at each pixel is preserved, little degradation of the hologram is expected.

In addition, we compared holograms designed by two different IFTAs versus phase compression

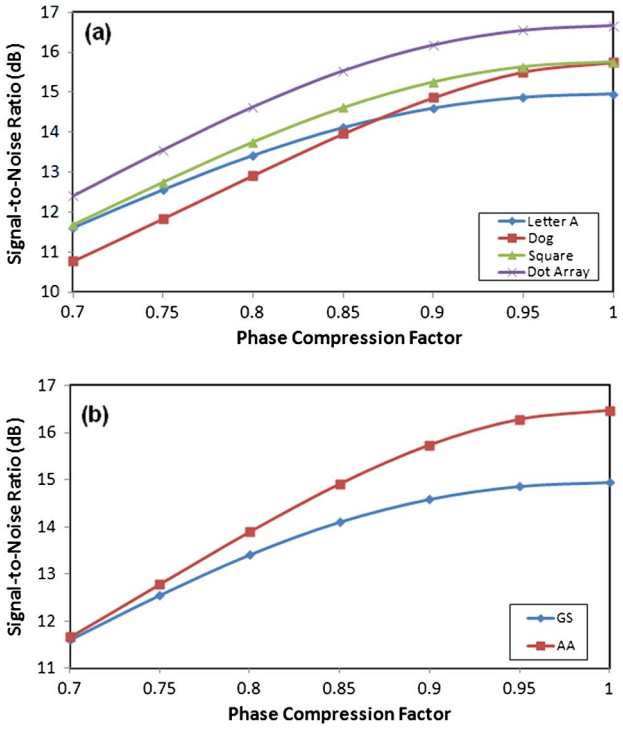

Fig. 8. (Color online) Degradation of signal-to-noise ratio (SNR) versus phase compression factor for (a) different target images, and (b) GS and AA algorithms for the binary letter "A" image.

factor, as shown in Fig. 8(b). For the binary letter "A," the modified AA algorithm showed better image quality (SNR = 16.47 dB) than the GS algorithm (SNR = 14.95 dB) before phase compression ($c = 1.0$). A larger decrease in SNR was observed for the modified AA algorithm of 2.6 dB versus 1.5 dB for the GS algorithm for $c = 0.8$. As phase compression was applied and c decreased, the SNR for the two algorithms converged.

The evolution of diffraction efficiency as a function of phase compression was studied for all cases, and typical data for the letter "A" image will be displayed. The diffracted power was partitioned into three regions for analysis: (1) the ZOD cancellation beam, (2) the image area, and (3) the black background area (excluding the corrective beam). The diffraction efficiency for the zero diffraction order domain is given by $\eta = ff^2$, where the optimum compression factor is found using Eq. (8). For example, for $ff = 0.9$, the diffraction efficiency to the zeroth order domain (sum of all three regions) is 81%. For c changing from 1.0 (no compression) to 0.9, the normalized power fraction in the image only decreased by 2.1%, as shown in Fig. 9. The corresponding change in the power in the dark background increased 1.2%. The generated ZOD beam contained less than 1.0% of the total power. As c decreased further, the majority of the power lost from the image was received by the ZOD corrective beam.

5. Conclusion

We demonstrated an efficient method to suppress the zero-order diffracted (ZOD) beam of holographic optical elements implemented using phase-only SLMs. The solution compressed the phase of the CGH globally, and thus the amplitude and phase of the corrective beam that canceled the ZOD beam could be adjusted using only two global parameters. This technique isolated the iterative, phase-only HOE pattern-generation process from that of cancellation beam formation. It reduced the computational complexity and time needed to arrive at an HOE with a compensated ZOD.

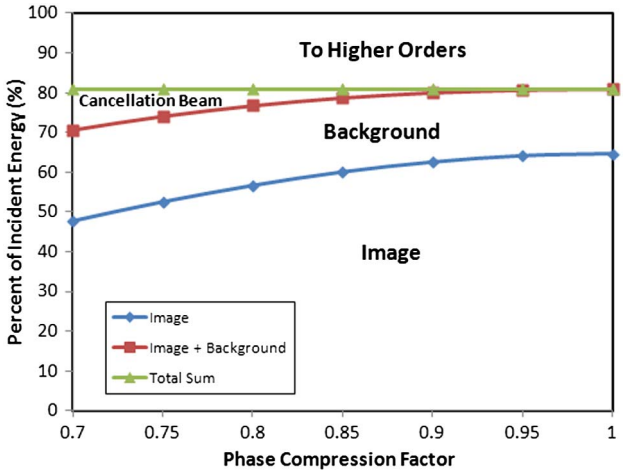

Fig. 9. (Color online) Simulated diffracted power versus phase compression factor.

We established the general model of the ZOD beam in the far field. The theoretical derivation proved that the ZOD and cancellation beam share the same functional form. The phase compression factor and rotation angle determine the amplitude and phase angle of the cancellation beam. Experimental results, using two reflective nematic liquid-crystal SLMs with different area fill factors, demonstrated a factor of 3 reduction of the ZOD beam power when using adaptive adjustment of the two compression parameters, c and θ. Our analysis concluded that the residual ZOD beam was from other contributions, such as imperfect SLM performance due to window reflections, calibration errors, interpixel cross talk, and device nonlinearity. The holographic image quality was maintained after phase compression was applied.

Various degrees of phase compression were simulated to examine the reconstructed image quality. The simulation result showed that the phase compressed HOE introduced a 1.5 to 2.8 dB image SNR degradation when using realistic SLM specifications, and a reasonably good image quality was preserved. In addition, the reconstructed image suffered little with respect to diffraction efficiency for a wide range of phase compression. In the future, we plan to apply this technique for ZOD suppression to Fresnel holograms for near-field image display.

Authors gratefully acknowledge Zhangjie Cao, Adam M. Crook, and Hari P. Nair for their valuable suggestion of the phase compression technique. The

authors also gratefully acknowledge support from the Office of Naval Research and the Army Research Office, with funding from the Defense Advanced Research Projects Agency (DARPA) Optical Lattice Emulator (OLE) program.

References

1. A. W. Lohmann and D. P. Paris, "Binary Frauhofer holograms, generated by computer," Appl. Opt. **6**, 1739–1748 (1967).
2. O. Ripoll, V. Kettunen, and H. P. Herzig, "Review of iterative Fourier-transform algorithms for beam shaping applications," Opt. Eng. **43**, 2549–2556 (2004).
3. J. Gillet and Y. Sheng, "Multiplexed computer-generated holograms with polygonal-aperture layouts optimized by genetic algorithm," Appl. Opt. **42**, 4156–4165 (2003).
4. J. Carpenter and T. D. Wilkinson, "Graphics processing unit–accelerated holography by simulated annealing," Opt. Eng. **49**, 095801 (2010).
5. G. Sinclair, J. Leach, P. Jordan, G. Gibson, E. Yao, Z. Laczik, M. Padgett, and J. Courtial, "Interactive application in holographic optical tweezers of a multi-plane Gerchberg-Saxton algorithm for three-dimensional light shaping," Opt. Express **12**, 1665–1670 (2004).
6. M. J. Thomson and M. R. Taghizadeh, "Design and fabrication of Fourier plane diffractive optical elements for high-power fibre-coupling applications," Opt. Lasers Eng. **43**, 671–681 (2005).
7. A. Moya, D. Mendlovic, J. Garcia, and C. Ferreira, "Projection-invariant pattern recognition with a phase-only logarithmic-harmonic-derived filter," Appl. Opt. **35**, 3862–3862 (1996).
8. S. Zwick, T. Haist, M. Warber, and W. Osten, "Dynamic holography using pixelated light modulators," Appl. Opt. **49**, F47–F58 (2010).
9. H. Zhang, J. Xie, J. Liu, and Y. Wang, "Elimination of a zero-order beam induced by a pixelated spatial light modulator for holographic projection," Appl. Opt. **48**, 5834–5841 (2009).
10. D. W. K. Wong and G. Chen, "Redistribution of the zero order by the use of a phase checkerboard pattern in computer generated holograms," Appl. Opt. **47**, 602–610 (2008).
11. D. Palima and V. R. Daria, "Holographic projection of arbitrary light patterns with a suppressed zero-order beam," Appl. Opt. **46**, 4197–4201 (2007).
12. R. W. Gerchberg and W. O. Saxton, "Practical algorithm for the determination of phase from image and diffraction plane pictures," Optik **35**, 237–250 (1972).
13. G. Milewski, D. Engström, and J. Bengtsson, "Diffractive optical elements designed for highly precise far-field generation in the presence of artifacts typical for pixelated spatial light modulators," Appl. Opt. **46**, 95–105 (2007).
14. J. W. Goodman, *Introduction to Fourier Optics*, 3rd ed. (Roberts & Co., 2005), pp. 103–108.
15. V. Kettunen, K. Jefimovs, J. Simonen, O. Ripoll, M. Kuittinen, and H. P. Herzig, "Diffractive elements designed to suppress unwanted zeroth order due to surface depth error," J. Mod. Opt. **51**, 2111–2123 (2004).
16. A. J. Caley, M. Braun, A. J. Waddie, and M. R. Taghizadeh, "Analysis of multimask fabrication errors for diffractive optical elements," Appl. Opt. **46**, 2180–2188 (2007).
17. S.-H. Lee and D. Grier, "Robustness of holographic optical traps against phase scaling errors," Opt. Express **13**, 7458–7465 (2005).
18. M. Duelli, L. Ge, and R. W. Cohn, "Nonlinear effects of phase blurring on Fourier transform holograms," J. Opt. Soc. Am. A **17**, 1594–1605 (2000).
19. Boulder Nonlinear Systems, "100% fill factor," http://bnonlinear.com/papers/new/100%20Fill%20Factor%20White%20Paper.pdf.
20. J. W. Goodman, *Introduction to Fourier Optics*, 3rd ed. (Roberts & Co., 2005), pp 82–84.
21. Boulder Nonlinear Systems, "XY format spatial light modulator date sheet," http://www.bnonlinear.com/products/xyslm/XYSeriesDS0909.pdf.
22. J. S. Liu and M. R. Taghizadeh, "Iterative algorithm for the design of diffractive phase elements for laser beam shaping," Opt. Lett. **27**, 1463–1465 (2002).